ECMI Modeling Week 2018
University of Novi Sad, Faculty of Technical Sciences

MODELING EFFECT OF TIME DELAY FOR LARGE NETWORK OF SEISMIC MONITOR

Christophe Picard University of Grenoble Alpes and Grenoble INP, France

Jordi Anguera	Autonomous University of Barcelona, Spain
Leevi Annala	University of Jyväskylä, Finland
Stefan Dimitrijevic	University of Novi Sad, Serbia
Patricia Pauli	Technical University of Darmstadt, Germany
Liisa-Ida Sorsa	Tampere University of Technology, Finland
Dimitar Trendafilov	University of Sofia "St. Kliment Ohridski", Bulgaria

Abstract

Seismic monitoring is used to study the behavior and composition of the underground floor. For earthquake prediction and underground works precise timing and positioning information is needed. Drilling companies use equipments that are linked in a network and are generally connected to a global positioning system for synchronization. However, instruments are not continuously synchronized and may deviate in time. Hence, the periods to which the vibration of the underground floor are caught might lack accuracy. Consequently, the precise localisation of the events becomes impossible. We have delay measurements and distance data available for an example seismic network and use it to correct the timing of the data in periods without GPS reception.

!!!TODO: Abstract was not in the original model, but it's stupid to not have one

August 3, 2018!!!TODO: CHANGE THIS TO THE DATE WHEN ITS READY

Contents

1 Introduction

In operation of seismic networks high quality of data is required for accurate prediction of seismic events. Precise timing is crucial but continuous GPS synchronization of the stations' internal clocks is not possible due to high energy consumption. This is why we need to detect time drifts differently in times of disconnection from the GPS in order to continuously guarantee reliable data.

The purpose of this work is to analyze noise in a large network of seismic monitors and to extract clock drift from the delay. This work suggests a way to determine clock drift based on the data only. For that, we use the information contained in the distance data to clear the delay data from clock drifts.

2 Problem Statement

2.1 Assumptions

All the stations have the same orientation. The medium the wave is propagating in is homogenous.

2.2 Definitions

Δ_i	clock drift at station i
δ_{ij}	Measured delay between station i and station j
$\hat{\delta}_{ij}$	Actual delay between station i and station j
ε_{ij}	Noise between two stations i and j, including clock drift and ambient noise
r_{ij}	Distance between stations
w_{ij}	Adjacency matrix element, weight between two nodes

2.3 Modelling time delay between seismic monitors

The network of monitors can be modelled as a complete graph. The signal of each monitor is cross-correlated with other monitor signals, finally yielding time-delay data $\hat{\delta}_{ij}$ between each monitor. The time delay between the monitors comprise information on the real time the seismic wave travels between the monitors δ_{ij}, the inaccuracies of the clock (time drift), and other noise affecting the measurement. The position of each seismic monitor in the network is available that can be used to compute the distances r_{ij} between all stations.

3 Data

The data is collected from a network of 73 seismic monitor stations recording ground vibrations in the Southeast region of France. The average distance between two monitors in the network is 166 km. The GPS coordinate position of each station in the network is known (Figure 1) and they each contain a clock which is synchronized to the GPS once a month. The seismic monitor sensor records compression and decompression as discrete values -1 and 1, respectively, every second. The sensor responds to any event in the area, be it an earthquake, tremor from road traffic, airplane or any other pressure wave which travels in the ground.

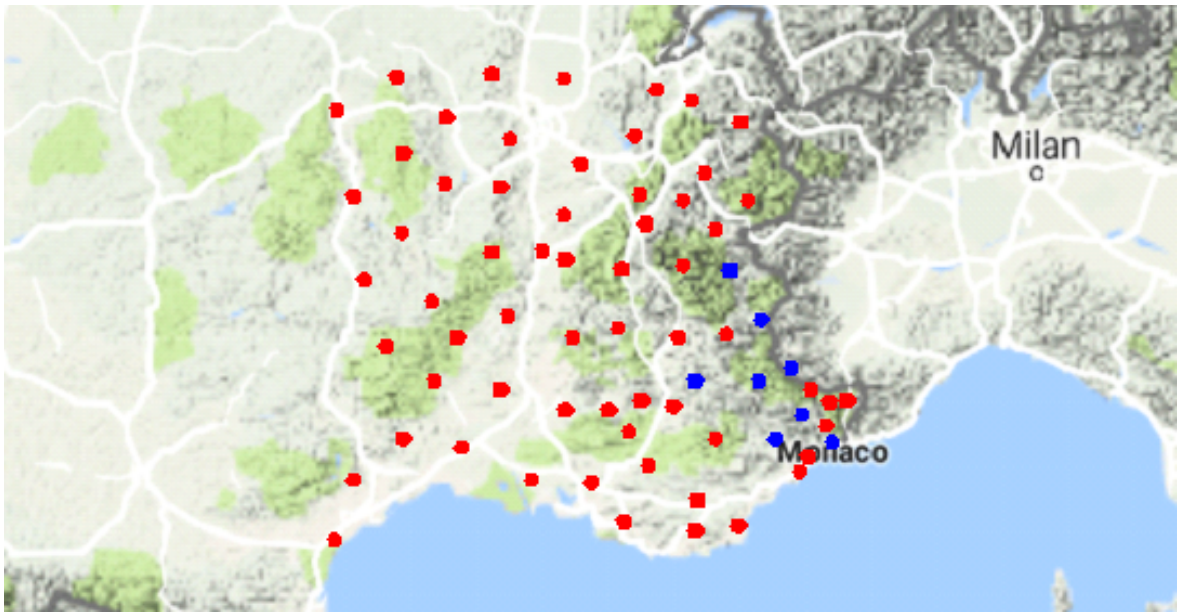

Figure 1: The network of seismic monitors are located in the Southeast France, mostly in the regions of Provence-Alpes-Côte d'Azur and Rhône-Alpes. The eight stations chosen as the small test set is shown as green in the southeast part of the area.

The stations work independent of each other and are occasionally shut down for some time frame for maintenance, repair or just random events. Just as occasionally they are brought back up to continue measuring. Therefore, the number of active stations varies over time. The Figure 2(a) shows the number of working stations, and the Figure 2(b) the number of working connections between the monitor stations over one year of measurements.

The compression and decompression data recorded by the stations is retrieved and run through initial data cleaning and filtering procedures. The data is then cross-correlated in one-hour time windows to yield time-delay data of signals between all monitors (Figure 3).

The time delays between monitors are assumed to depend on the distance between the those same monitors. The further away the monitors are from each other, the longer

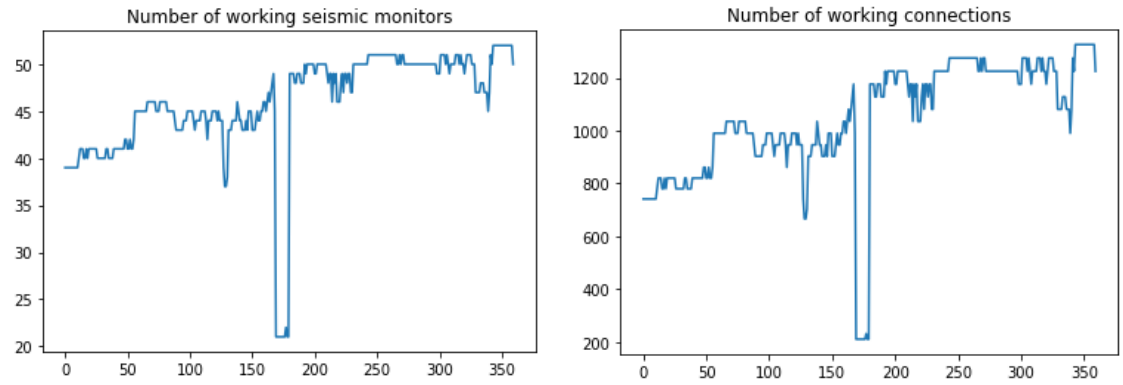

(a) The number of working seismic monitor stations.

(b) The number of working connections between the stations.

Figure 2: Working stations and connections over one year time period.

the time a seismic wave travels from one station to another. The time the wave travels corresponds to the actual delay and is the lion share of the measured delay between stations. Noise and clock drift are of a lower in order of magnitude. Figure 4 shows the time signal of the station pairs that are closest and furthest apart over a time frame of 10 days supporting this assumption. One can see that the variance of the delays is much higher for the stations that are far apart. However the seismic events occur randamly.

The Figure 5 shows an example of time-delay evolution of all monitors over 24 hours. The distributions are symmetric with zero mean which implies that the delays at an instant cancel out over the whole area the 73 stations are mounted in. The interesting feature of the histograms is how the shape of the distribution changes slowly over time. However, the mean remains zero.

3.1 The most influential stations

The stations playing a key role in the global deviation of the total graph will be evaluated by the singular value decomposition of the global delays matrix $\hat{\boldsymbol{\delta}} \in \mathbb{R}^{n \times m}$, where n is the number of edges and m the number of time steps. !!!TODO: check the notation for the number of edges and time steps

In order to find the index of the eigenvector with the most relative importance by the number of connections (regardless of the observed time delays) the time delay matrix $\hat{\boldsymbol{\delta}}$ was turned binary.

The Figure 6(a) shows the relative weight of the connections for each of the eigenvalue's index, the first one being the largest one. With that, the next step was to find the connections with the largest relative weight and the limit at which the connections do not have any more influence in the overall time delay, which will be shown in Figure

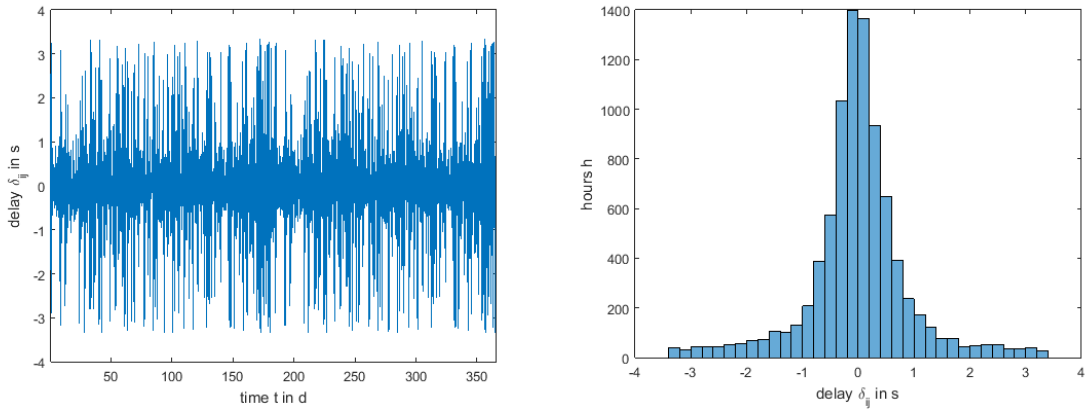

(a) Time Signal. (b) Histogram.

Figure 3: The time-delay signal recorded between one station pair over a year. The time delay is computed in one-hour windows, yielding 24 time-delay values over a day.

6(b) as a plot of the relative weight of each of the connections using the matrix $\hat{\boldsymbol{\delta}}$ with the measured time delays.

In order to select the group of connections with the largest weight a threshold of $|0.05|$ was taken, which resulted in 74 connections among 52 active stations. Finally, three stations with the largest numbers of connections (34, 21, and 13) were identified. The remaining stations had only two connections or less.

These three stations were identified as the most influential stations, along with another group of five nearby these three stations stations, were taken as a small test set of stations to evaluate the methods developed in this work.

4 Methods

Let $\hat{\boldsymbol{\delta}} \in \mathbb{R}^{n \times n}$ be the measured pairwise time delays of the system, $\boldsymbol{\delta}$ the actual pairwise time delays, and $\boldsymbol{\varepsilon}$ an error term including clock drift of the station's clock and other errors

$$\hat{\boldsymbol{\delta}} = \boldsymbol{\delta} + \boldsymbol{\varepsilon}. \tag{1}$$

Each of the monitors are equipped with a clock which runs independent of others. It is synchronized via GPS system once a month and then runs independently. The inaccuracy in timing events at a station is caused by variations in the clocks' oscillators which oscillation may not be idea, they might respond to outside events and the oscillations are also affected by earthquakes.

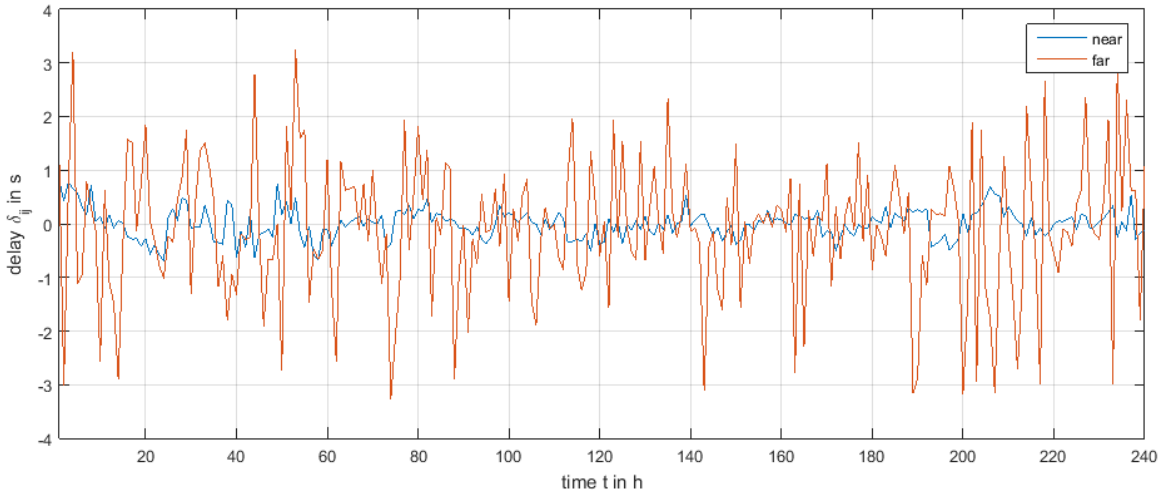

Figure 4: Comparison of the delay of the furthest and closest station pairs over 10 days.

The position of each seismic monitor in the network is known. As the monitors are spread across a large area, it is assumed that local tremors are detected by stations that are close by, and therefore the correlations found in the pairwise cross-correlations and time delay data between them have higher likelihood to be linked.

4.1 The graph denoising model

4.1.1 Definitions

The computational denoising model developed in this work involves weighted network estimation by the use of topological graph metrics, described in detail in Spyrou and Escudero 2017.

The monitor network constitutes a weighted graph $\mathcal{G}_\delta = (\mathcal{V}, \mathcal{E}, \hat{\boldsymbol{\delta}}_t)$ defined by a finite set of nodes $\mathcal{V}$ with $|\mathcal{V}| = n$, a set of edges $\mathcal{E} = \{(v_i, v_j) \in \mathcal{E}\}$, with $\max|\mathcal{E}| = n^2 - n$ and the weighted adjacency matrix $\hat{\boldsymbol{\delta}}$ with $\hat{\delta}_{ii} = 0$ for all i based on the measured time delays between stations. The matrix $\hat{\boldsymbol{\delta}}$ is symmetric and describes the time delays between events in the graph, and is normalized, i.e. $\hat{\delta}_{ij} \in [0, 1]$. The weighted adjacency matrix indicates the strength of connection between nodes.

The network also specifies another weighted graph $\mathcal{G}_r = (\mathcal{V}, \mathcal{E}, \boldsymbol{W})$, which sets of nodes and edges are the same as those of $\mathcal{G}_\delta$, but the adjacency weight matrix $\boldsymbol{W}$ is based on the physical distances between the station pairs. Also these weights are normalized between $[0, 1]$.

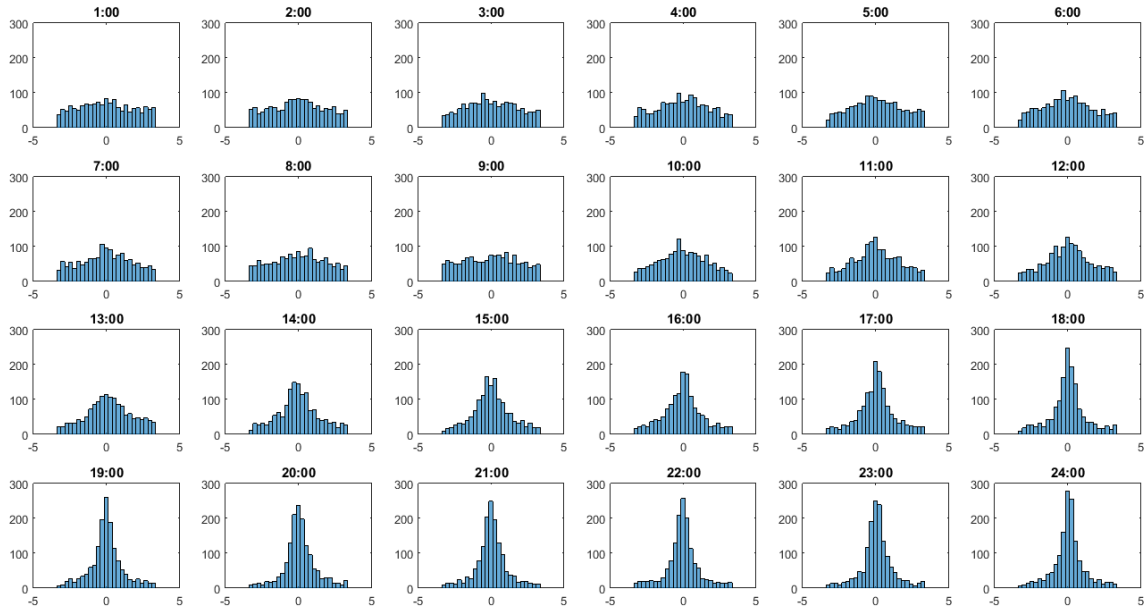

Figure 5: Histograms of time delays of all active stations recorded over 24 hours. The histogram shows how many connections have a particular delay at the instant.

4.1.2 Graph metrics

Graph metrics are scalar functions of the weight matrix $\boldsymbol{X}$ of a graph

$$f_i(\boldsymbol{X}) = K_i \tag{2}$$

They quantify a property of the network. In this work, the metrics involve time delays (δ_{ij}) or the physical distances (r_{ij}) between stations. The connection strength of a node i that is the row sum of the normalized weighted adjacency matrix:

$$f_i(\hat{\boldsymbol{\delta}}) = \sum_j \hat{\delta}_{ij} \qquad \text{for } \mathcal{G}_\delta = (\mathcal{V}, \mathcal{E}, \hat{\boldsymbol{\delta}}_t) \tag{3}$$

$$K_i = f_i(\boldsymbol{W}) = \sum_j w_{ij} \quad \text{for } \mathcal{G}_r = (\mathcal{V}, \mathcal{E}, \mathbf{W}). \tag{4}$$

The connection strength can be interpreted as the sum of all normalized delays of all of the connections to node i.

Figure 7 shows a minimal example of how the metric is computed. The node 1 has three connections yielding a connection strength $w_{12} + w_{13} + w_{14} = 0.1 + 0.3 + 0.6 = 1.0$. The other nodes and their connection strengths are computed similarly.

Next, we look at the K_i. Since we have the distance measurements available and expect a correlation between the delays and distances, we want to use this information to

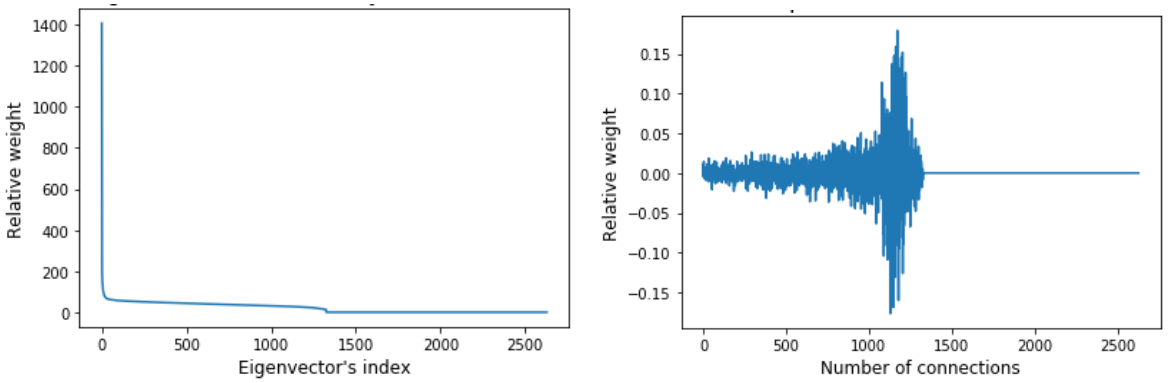

(a) Singular values for the binary connection matrix. (b) Influences of connections.

Figure 6: Determining the influences of connections.

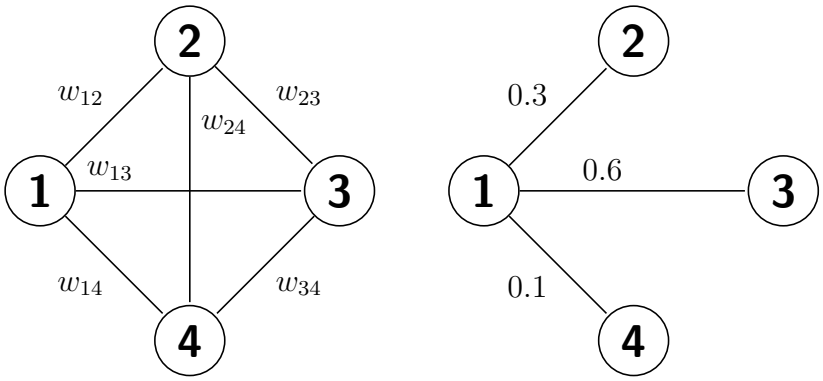

Figure 7: Minimal example to help understand the computation of graph metrics.

denoise the delay measurements and define

$$K_i = f_i(\mathbf{W}). \tag{5}$$

It is the connection strength as well. But here we plug in the distance matrix $\mathbf{W}$. The distances are constants and yield constant K_i. The weight matrix $\mathbf{W}$ is a function of the distance between node i and node j.

1. First, we choose the function to be the reciprocal of the distances of the node to all other nodes, $w_{ij} = 1/r_{ij}$, normalized between $[0, 1]$. Higher values correspond to nodes with short distances to all other nodes.

2. Second, we try a metric with weights proportional to the distances ($w_{ij} \propto r_{ij}$), normailzed between $[0, 1]$ accordingly. Here, high values correspond to long distances between two stations.

Other possible metrics are average neighbor degrees (resilience), transitivity, or a clustering coefficient. The analysis based on these metrics is beyond the scope of this work.

4.1.3 Cost function

We assume to have estimates of M differentiable graph metrics, one for each node i, of the original matrix $\hat{\boldsymbol{\delta}}$, i.e. $f_i(\hat{\boldsymbol{\delta}}) = K_i$, where $i \in \{1, \ldots, M\}$, then we can formulate a cost function that measures the deviation of the observed weight matrix's metrics $f_i(\hat{\boldsymbol{\delta}})$ to the estimates K_i as:

$$c(\hat{\boldsymbol{\delta}}) = \sum_i e_i^2(\hat{\boldsymbol{\delta}}) = \sum_i (f_i(\hat{\boldsymbol{\delta}}) - K_i)^2 \tag{6}$$

The error is minimized with gradient descent updates on $\hat{\boldsymbol{\delta}}$:

$$\hat{\boldsymbol{\delta}}^{(k+1)} = \hat{\boldsymbol{\delta}}^k - \mu \sum_i e_i(\hat{\boldsymbol{\delta}}^k) \frac{df_i(\hat{\boldsymbol{\delta}}^k)}{d\hat{\boldsymbol{\delta}}^k}, \tag{7}$$

where k is the iteration index and μ the learning rate. We find the derivative for the gradient descent update step. For $i = 2$ it is

$$\frac{df_2}{d\boldsymbol{\delta}} = \frac{\sum_j \hat{\delta}_{2j}}{d\hat{\boldsymbol{\delta}}} = \begin{bmatrix} 0 & 1 & 0 & \ldots & 0 \\ 1 & 0 & 1 & \ldots & 1 \\ 0 & 1 & 0 & \ldots & 0 \\ \vdots & \vdots & \vdots & \ddots & \vdots \\ 0 & 1 & 0 & \ldots & 0 \end{bmatrix}. \tag{8}$$

It is a symmetric matrix with ones in the ith row and ith column. The diagonal entries remain zero.

4.2 Clock drift estimate

The denoising model in section 4.1 computes the denoised estimate $\boldsymbol{\delta}$ of the measurement data $\hat{\boldsymbol{\delta}}$. The algorithm is run over a series of time points and an estimate for the clock drift Δ_{ij} between each station pair is obtained.

The noise, ε_{ij}, between each pair between two stations in the system is caused by clock drifts Δ_i and Δ_j, and other ambient errors E_{ij}

$$\varepsilon_{ij} = \Delta_i - \Delta_j + E_{ij}. \tag{9}$$

The unwanted ambient noise E_{ij} is assumed to be white noise that can be cancelled out by interpolation of the total noise.

The clock errors of individual stations can be written in matrix form

$$\begin{bmatrix} 1 & -1 & 0 & 0 & \dots & 0 \\ 1 & 0 & -1 & 0 & \dots & 0 \\ 1 & 0 & 0 & -1 & \dots & 0 \\ \vdots & \vdots & \vdots & \vdots & \ddots & \vdots \\ 1 & 0 & 0 & 0 & \dots & -1 \\ 0 & 1 & -1 & 0 & \dots & 0 \\ 0 & 1 & 0 & -1 & \dots & 0 \\ 0 & 1 & 0 & 0 & \ddots & 0 \\ \dots & \dots & \dots & \dots & \dots & \dots \\ 0 & 0 & \dots & 0 & 1 & -1 \end{bmatrix} \begin{bmatrix} \Delta_1 \\ \Delta_2 \\ \Delta_3 \\ \Delta_4 \\ \vdots \\ \Delta_k \\ \vdots \\ \Delta_{n-1} \\ \Delta_n \end{bmatrix} = \begin{bmatrix} \Delta_1 - \Delta_2 \\ \Delta_1 - \Delta_3 \\ \Delta_1 - \Delta_4 \\ \vdots \\ \Delta_1 - \Delta_n \\ \Delta_2 - \Delta_3 \\ \Delta_2 - \Delta_4 \\ \vdots \\ \Delta_2 - \Delta_k \\ \vdots \\ \Delta_{n-1} - \Delta_n \end{bmatrix} = \begin{bmatrix} \Delta_{12} \\ \Delta_{13} \\ \Delta_{14} \\ \vdots \\ \Delta_{1n} \\ \Delta_{23} \\ \Delta_{24} \\ \vdots \\ \Delta_{2k} \\ \vdots \\ \Delta_{(n-1)n} \end{bmatrix},$$

which can be written more compactly as

$$\mathbf{Gs} = \mathbf{m} \tag{10}$$

where s is the unknown model vector and m the known data Sens-Schonfelder 2008. The matrix $\mathbf{G}$ has rank $n-1$, meaning that it is lacking full rank.

This represents a classical overdetermined inversion problem which can be solved by ordinary least squares regression after Tikhonov requlariza tion. The ordinary least squares seeks to minimize the sum of squared residuals

$$\|\mathbf{Gs} - \mathbf{m}\|_2^2. \tag{11}$$

When Tikhonov regularisation is added to the Equation 11, we obtain

$$\|\mathbf{Gs} - \mathbf{m}\|_2^2 + \|\mathbf{\Gamma s}\|_2^2, \tag{12}$$

for some suitable Tikhonov matrix $\mathbf{\Gamma}$. We choose this matrix as a multiple of the identity matrix $\mathbf{\Gamma} = \alpha\mathbf{I}$, giving preference to smaller norms.

The explicit solution is hence given by

$$\hat{\mathbf{s}} = (\mathbf{G}^T\mathbf{G} + \mathbf{\Gamma}^T\mathbf{\Gamma})^{-1}\mathbf{G}^T\mathbf{m}. \tag{13}$$

4.3 Algorithm

The graph denoising algorithm by Spyrou and Escudero 2017 is described in algorithm 1.

Data: Noisy data W_e,
calculated estimates for graph metrics K_m,
learning rate μ,
maximum error ϵ
Result: Denoised data $\hat{W}$
initialization: $t = 0$, $W_0 = W_e$, $E = \sum_m (f_m(W_0) - K_m)^2$
while $E > \epsilon$ **do**
  $W_{(t+1)} = W_t - \mu \sum_m (f_m(W_t) - K_m) \frac{df_m(W_t)}{dW_t}$
  if $w_{i,j} < 0$ **then**
    $w_{i,j} = 0$
  end
  if $w_{i,j} > 1$ **then**
    $w_{i,j} = 1$
  end
  $E = \sum_m (f_m(W_{t+1}) - K_m)^2$
  $t = t + 1$
end
$\hat{W} = W_t$

Algorithm 1: Graph denoising algorithm.

The algorithm for obtaining the time delays for the measuring stations during time t is described in algorithm 2.

Data: Results from algorithm 1, δ,
measured time delays, $\hat{\delta}$, and
Tikhonov regularisation constant, α.
Result: Clock drifts Δ_i
get the error matrix ε between the stations by $\hat{\delta} - \delta$.
arrange the error matrix ε to match m from equation 10 and call it m.
$\Delta = (G^T G + \alpha^2 I^T I)^{-1} G^T m$, where G comes from equation 10, and I is identity matrix of the size of $G^T G$.

Algorithm 2: Clock drift calculation.

5 Results

5.1 Signal denoising

5.2 Clock deviations

6 Conclusions and Outlook

By analyzing the delay data we clearly showed that it changes over time showing patterns other than only white noise. This is due to clock drift. We used a method of weighted network estimation by the use of topological graph metrics exploiting the relation between delay and distances to denoise the data. The method is robust to temporarily disconnected stations that are only included as they are only included in the calculations when they are active. Hence, the algorithm can be run for on larger networks. The algorithm produced denoised delays we could deduce clock drifts from. Due to missing validation data we cannot make conclusions on the quality of our estimates. The algorithm could either be run on synthetic data where the results are known or on data sets that include continuous GPS synchronized data. To get more compelling results other metrics could be used, or even a combination of multiple metrics.

7 Group work dynamics

The student group should write an assessment of the group work dynamics (including both the Modeling Week time itself and the time/workload afterwards, spent on writing the report itself). In particular, you should at least answer to the following questions:

- How did you plan the work?
- How was the work distributed between the partners?
- What was beneficial or challenging about the group work?

Christophe gave us a more detailed presentation of the problem in the first group work session. After this, we asked questions and started a first discussion. From then on Christophe left the work and work distribution to us. We started by all absorbing the problem individually reading papers. The same afternoon we used the blackboard to discuss our ideas and find a feasible starting point for our work. Christophe had given us some assumptions and questions. The second day we decided to sit closer together in a circle and be closer to the blackboard that we kept using throughout the whole week to brainstorm ideas. We let everyone individually decide what they wanted to

work on and sometimes asked aorund what everyone was currently working on to have a good overview and avoid that anything was left aside or the same thing was done twice. One subteam works on the methods and developed the applied metrics, others analyzed the data and performed single value decomposition. Some team members had more experience in group works than others and everyone had different backgrounds. This was an advantage in terms of the various view points and abilities we had as a group. However, communication was sometimes difficult as we didn't know what to expect from each other.

8 Instructor's assessment

Every instructor is asked to add a brief (1–2 paragraph) summary of how the group has performed through the week, especially with respect to the problem's initial goals and the actual achievements. Here is also the place to report possible total or part-time absences of the students during the group work hours — these can be also reported by the fellow group mates.

References

Sens-Schonfelder, Christoph (2008). "Synchronizing seismic networks with ambient noise". In: *Geophysical Journal International* 174.3, pp. 966–970. DOI: 10.1111/j.1365-246X.2008.03842.x. eprint: /oup/backfile/content_public/journal/gji/174/3/10.1111/j.1365-246x.2008.03842.x/3/174-3-966.pdf. URL: http://dx.doi.org/10.1111/j.1365-246X.2008.03842.x.

Spyrou, Loukianos and Javier Escudero (2017). "Weighted network estimation by the use of topological graph metrics". In: *CoRR* abs/1705.00892. arXiv: 1705.00892. URL: http://arxiv.org/abs/1705.00892.